Published in IET Signal Processing
Received on 10th November 2009
Revised on 22nd June 2010
doi: 10.1049/iet-spr.2009.0267

ISSN 1751-9675

Improved parametric families of intersymbol interference-free Nyquist pulses using inner and outer functions

S.D. Assimonis[1] *M. Matthaiou*[2,4] *G.K. Karagiannidis*[1] *J.A. Nossek*[3]

[1]*Department of Electrical and Computer Engineering, Aristotle University of Thessaloniki, 54 124 Thessaloniki, Greece*
[2]*Technische Universität München (TUM), Arcistrasse 21, 80333 Munich, Germany*
[3]*Institute for Circuit Theory and Signal Processing, Technische Universität München (TUM), Arcistrasse 21, 80333 Munich, Germany*
[4]*Department of Signals and Systems, Chalmers University of Technology, SE-412 96 Gothenburg, Sweden*
E-mail: michail.matthaiou@chalmers.se

Abstract: In this article, the authors introduce and study the performance of two novel parametric families of Nyquist intersymbol interference-free pulses. Using only two design parameters, the proposed pulses yield an enhanced performance compared to the sophisticated flipped-inverse hyperbolic secant (asech) filter, which was recently documented in the literature. Although the construction of parametric families originates from the work of Beaulieu and Damen, the authors' approach is based on the concept of 'inner' and 'outer' functions and for this reason a higher flexibility in the choice of the family members is achieved. The proposed pulses may decay slower than the original raised-cosine (RC) pulse outside the pulse interval, but exhibit a more pronounced decrease in the amplitudes of the two largest sidelobes and this accounts for their improved robustness to error probabilities. It is clearly shown, via simulation results, that a lower bit error rate (BER), compared to the existing pulses, can be achieved for different values of the roll-off factor and timing jitter. Moreover, a smaller maximum distortion as well as a more open-eye diagram are attained which further demonstrate the superiority of the proposed pulse shaping filters.

1 Introduction

It is an indisputable fact that the rapid evolution of wireless communications over the last few decades has imposed new demands for better bandwidth reuse and higher error-free data rates. Since the pioneering work of Nyquist in the late 1920s [1], an extensive amount of research and industry interest has been devoted to the development of intersymbol interference (ISI)-free pulses that guarantee the highly desirable distortionless transmission, that is, minimum number of errors. Apart from the ISI-free prerequisite, pulse shaping filters have to exhibit low sensitivity to timing errors [2]. The most popular pulse that fulfils both conditions is the so-called raised-cosine (RC) pulse that has found numerous applications in the area of digital communications. Nevertheless, in practical receivers the presence of timing jitter causes the actual sampling points to deviate from the optimal positions leading to symbol timing errors. This, in turn, implies that the pulse tails must decay as quickly as possible outside the pulse interval so that the undesired effects of jitter are eliminated. In addition, taking into account that the great majority of current practical systems are band limited along with the steadily increasing spectrum congestion [3], it becomes apparent that the system designer has to convey the highest possible error-free data rate within a fixed limited bandwidth. Normally, a trade-off exists between increased data rate and time-domain tail suppression [2, 4].

In order to meet all the above-mentioned constraints, a plethora of alternatives have been reported in the corresponding literature. For instance, in [5] the so-called Beaulieu or better than raised-cosine (BTRC) pulse, which outperforms the RC pulse in terms of larger eye opening and smaller average symbol error rate, was proposed. This performance enhancement was observed even though the tails of BTRC asymptotically decay as $1/t^2$, whereas those of RC as $1/t^3$. This interesting phenomenon can be attributed to the fact that the two main sidelobes' amplitudes of BTRC are smaller than the larger sidelobes' amplitudes of RC. Please note that the BTRC pulse remains the best-known pulse with an explicit closed-form formula in the time domain. The authors in [6], developed the so-called 'flipped-hyperbolic secant' (fsech) and 'flipped-inverse hyperbolic secant' (asech) pulses; the latter performs even better than the BTRC and yields a smaller maximum distortion and also remains robust to root and truncation operations. (In the original paper [6], this pulse was referred to as farcsech. We use the name asech instead for the continuity of notation throughout the paper.) Please note that throughout the paper it will be our reference pulse

since, to the best of our knowledge, yields the best performance compared to any other pulse available in the corresponding literature with only two fixed design parameters.

The pulse family presented in [7] constitutes a radically new approach to the implementation of ISI-free pulses; in particular, any member of the proposed family represents a nth degree polynomial where the asymptotic decay rate is related to n as $\lfloor(2n+5)/3\rfloor$, with the symbol $\lfloor\cdot\rfloor$ denoting the floor function. The pulse was shown to outperform all the aforementioned pulses but, at the same time, required the optimisation of n design parameters (polynomial coefficients). As such, there is not a unique, explicit formula for a pulse which will systematically outperform BTRC and asech pulses for all values of the roll-off factor and timing jitter. Likewise, the family of pulses proposed by Alexandru [8] (superposition of a linear term with two sine harmonic terms) relies on a rough non-optimal search to select the best design parameters. We also refer to the linear combination of the RC and BTRC pulses, originally proposed in [9], which was demonstrated to systematically outperform the BTRC and asech pulses but its advantages diminish as the roll-off factor and sampling time errors increase.

From the previous discussion it must have become clear that a pulse with the minimum number of design parameters that need to be optimised for different values of the roll-off factor and timing jitter, and the smallest bit error rate (BER) for any arbitrary value of the roll-off factor and sampling time error, represents the key goal in the design of practical receivers. Note that the number of filter parameters affects only the complexity of the design/optimisation process, which is carried out offline, and does not intervene with the digital implementation of such filters. In this light, two novel parametric ISI-free families are presented herein with only two design parameters that exhibit better error performance and a more open eye diagram than the sophisticated asech pulse. Equally importantly, it is shown that the latter is a member of the first proposed family which in practice means that the proposed family represents a generalisation of the work presented in [6]. In addition, we demonstrate that most members of the two families offer an improved performance not only in terms of error rate but also of maximum distortion and eye diagram. The presented results complement some of our recent investigations (e.g. [10, 11]) and provide a systematic theoretical framework for the design of robust Nyquist pulses.

The starting point of the analysis presented herein has been the seminal work carried out by Beaulieu and Damen [12]. In their analysis, the authors proposed a parametric family of Nyquist ISI-free pulses based on a spline frequency-domain pattern with the main advantage lying on the high flexibility in the pulse design. The members of this family have an even and real frequency spectrum which implies that the time pulse is real valued and even, respectively. However, the flexibility in finding the optimum pulse for each specific application is a result of a third free parameter which increases the degrees of freedom, thereby making most of the known ISI-free pulses represent special cases of this generalised family.

The remainder of the paper is organised as follows: in Section 2, we introduce the two parametric families of ISI-free pulses in the frequency domain, whereas Section 3 is oriented to their time-domain characteristics and in particular to the decay rate of the filters' sidelobes. In Section 4, the performance of both families is evaluated from different practical perspectives of interest. Finally, Section 5 concludes the paper and summarises the key findings.

2 Parametric families of ISI-free pulses using inner and outer functions

The proposed families have been built upon the notions of inner and outer functions which find numerous applications, spanning wavelet theory to image compression and modelling of microwave circuits [13]. As was previously highlighted, the initial application of composite functions to the problem of filter design can be found in [12]. In the present case, the main concept for the filter construction can be summarised as follows:

1. Choose an outer function $g(f)$ so that it only needs to be continuous and differentiable in the frequency interval $B(1-\alpha) \le |f| \le B(1+\alpha)$ and, most importantly, its frequency response retains a convex shape in the interval $B(1-\alpha) < |f| \le B$ and concave in $B < |f| \le B(1+\alpha)$. The latter prerequisite guarantees the convexity of the filters' responses in $B(1-\alpha) < |f| \le B$ that comes in fundamental contrast with the concave responses of the conventional filters, like RC and fsech. Two candidate outer functions that fulfil the aforementioned conditions are the well-known inverse cosine and inverse hyperbolic secant functions which can be denoted as $g(f) = \text{acos}(f)$ and $g(f) = \text{asech}(f)$, respectively.
2. Once the outer function $g(f)$ has been chosen, the different choices of the inner functions $h(f)$ represent essentially trade-offs between the decay rate and the sidelobes' amplitudes and for this reason yield different BERs and eye diagrams. Then, the composite filter response can be written as $\mathcal{G}(f) = g(h(f))$. The conditions $h(f)$, and in turn $\mathcal{G}(f)$, have to fulfil are the following: (a) the solution of the equation $\mathcal{G}(f) = 0$ should be real and different than zero and (b) the parameter γ, defined later in (2), must be real or imaginary but not complex.

For the first proposed family of filters, three different alternatives (members) are introduced, according to $h(f) = \text{acos}(f)$, $h(f) = \text{asech}(f)$ and $h(f) = \log(f)$. Then, the total filter's frequency response reads as (see (1))
where α denotes the roll-off factor ($0 \le \alpha \le 1$), determining the bandwidth occupied by the pulse and the time-domain tail suppression, and $B = 1/(2T)$ is the Nyquist frequency

$$S_1(f) = \begin{cases} T, & |f| \le B(1-\alpha) \\ T\left\{1 - \frac{1}{2\gamma}\mathcal{G}\left(\frac{\gamma_0}{2\alpha B}(-|f| + B(1+\alpha))\right)\right\}, & B(1-\alpha) < |f| \le B \\ T\left\{\frac{1}{2\gamma}\mathcal{G}\left(\frac{\gamma_0}{2\alpha B}(|f| - B(1-\alpha))\right)\right\}, & B < |f| < B(1+\alpha) \\ 0, & B(1+\alpha) \le |f| \end{cases} \quad (1)$$

doi: 10.1049/iet-spr.2009.0267

and T the repetition rate (transmission symbol period). The parameters γ and γ_0 are defined directly through the inverse $\mathcal{G}$ function according to

$$\gamma_0 = \mathcal{G}^{-1}(0) \quad \text{and} \quad \gamma = \mathcal{G}\left(\frac{\gamma_0}{2}\right) \tag{2}$$

This choice ensures the continuity of $S(f)$ within the considered interval $[0, B(1+\alpha)]$ and further at the key transition points

$$f = B(1-\alpha), \quad f = B \quad \text{and} \quad f = B(1+\alpha) \tag{3}$$

the obtained values are, respectively

$$S(B(1-\alpha)) = 1, \quad S(B) = 1/2 \quad \text{and} \quad S(B(1+\alpha)) = 0 \tag{4}$$

It should be noted that the asech pulse is by definition a special member of this family, obtained directly as $\mathcal{G}(f) = \text{asech}(f)$. In a similar manner we obtain the acos pulse as $\mathcal{G}(f) = \text{acos}(f)$, with $\mathcal{G}(f)$ being the inverse function of $\cos(f)$. Henceforth, each family member will be denoted via the outer and inner functions, separated by brackets, that is, acos[acos] and so on. The frequency responses of all the possible combinations are depicted in Figs. 1*a* and *b* for a roll-off factor $\alpha = 0.35$.

On the other hand, the second proposed family has only two members and the exponential function as the inner function. The main reason behind developing this separate family was the fact that when $h(f) = \exp(f)$ we readily obtain $\gamma_0 = 0$, which leads to the degeneration of (1) into a rectangular pulse in the interval $[-B, B]$. Hence, in order to circumvent this undesired implication, we also propose a second class of Nyquist filters, that is (see (5))
where $\gamma = \mathcal{G}(1/2)$.

The parameters γ and γ_0 are summarised in Table 1. In addition, the frequency response of the second family is illustrated in Fig. 2. As was previously mentioned, both $S_1(f)$ and $S_2(f)$ have a convex shape in the interval $B(1-\alpha) < |f| \le B$ and concave in the interval $B < |f| \le B(1+\alpha)$, in order to allow for an amount of energy to be transferred in the high spectral region. The only exception is the asech[log] pulse whose response is semi-convex and semi-concave in the corresponding regions. (This can be visually seen by considering the straight line connecting $(B(1-\alpha), 1)$ with $(B(1+\alpha), 0)$.) We recall that the RC pulse as well as the fsech pulse [6] have reversely a convex shape in $B(1-\alpha) < |f| \le B$ and concave in $B < |f| \le B(1+\alpha)$. This key difference accounts for the proposed pulses exhibiting weaker sidelobes in the time domain and therefore offering an improved robustness against the time-jitter effects, compared to the conventional pulses.

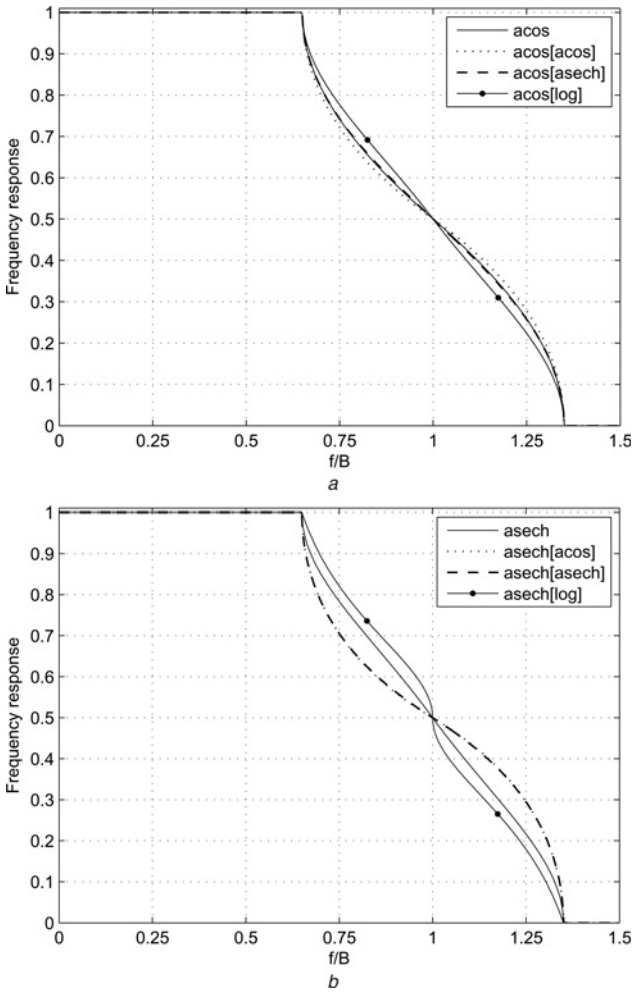

Fig. 1 *Frequency-domain responses of the first parametric family (acos and asech filters) with roll-off factor $\alpha = 0.35$*

a Acos filters
b Asech filters

3 Time-domain characteristics

In this section, the time-domain characteristics of the two considered families are explored with a view to their decay rate and tail suppression. In order to estimate how rapidly the tails of the pulses decay in time, we start with a theorem introduced previously in [12], which is rewritten here for the sake of completeness.

Theorem 1 ([12]): If the first $m-1$ derivatives of $S_i(f)$ $(i = 1, 2)$ are continuous and the mth derivative of $S_i(f)$ has one or more amplitude discontinuities then $|s_i(t)|$ decays as $1/|t|^{m+1}$ when $|t|$ is large.

Using this theorem as a starting point we show that the following lemma is fulfilled

$$S_2(f) = \begin{cases} T, & |f| \le B(1-\alpha) \\ T\left\{1 - \dfrac{1}{2\gamma}\mathcal{G}\left(\dfrac{1}{2\alpha B}(|f| - B(1-\alpha))\right)\right\}, & B(1-\alpha) < |f| \le B \\ T\left\{\dfrac{1}{2\gamma}\mathcal{G}\left(\dfrac{1}{2\alpha B}(-|f| + B(1+\alpha))\right)\right\}, & B < |f| < B(1+\alpha) \\ 0, & B(1+\alpha) \le |f| \end{cases} \tag{5}$$

Table 1 Design parameters γ and γ_0 of all filters

Pulse	γ_0	γ
acos	1	$\pi/3$
acos[acos]	$\cos(1) = 0.5403$	$\text{acos}\left(\text{acos}\left(\frac{\cos(1)}{2}\right)\right) \simeq 0.7531e^{j\pi/2}$
acos[asech]	$\text{sech}(1) \simeq 0.6481$	$\text{acos}\left(\text{asech}\left(\frac{\text{sech}(1)}{2}\right)\right) \simeq 1.188e^{j\pi/2}$
acos[log]	e	$\text{acos}\left(\log\left(\frac{e}{2}\right)\right) \simeq 1.2589$
asech	1	asech(1/2)
asech[acos]	$\cos(1) \simeq 0.5403$	$\text{asech}\left(\text{asech}\left(\frac{\cos(1)}{2}\right)\right) \simeq 0.6906e^{j\pi/2}$
asech[asech]	$\text{sech}(1) \simeq 0.6481$	$\text{asech}\left(\text{asech}\left(\frac{\text{sech}(1)}{2}\right)\right) \simeq 0.9791e^{j\pi/2}$
asech[log]	e	$\text{asech}\left(\log\left(\frac{e}{2}\right)\right) \simeq 1.8501$
acos[exp]	1	$\text{acos}(\sqrt{e}) \simeq 1.085e^{j\pi/2}$
asech[exp]	1	$\text{asech}(\sqrt{e}) \simeq 0.9191e^{j\pi/2}$

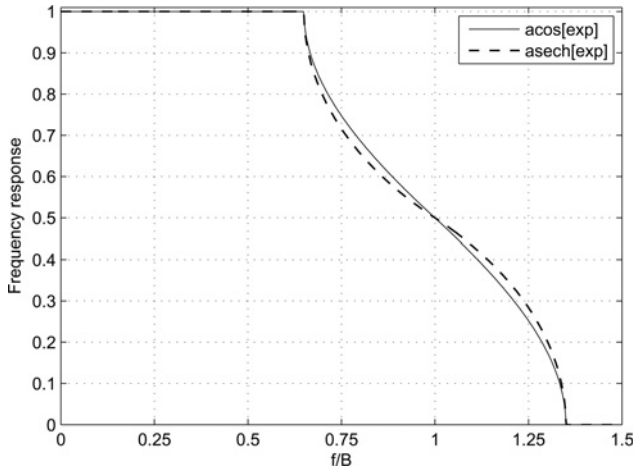

Fig. 2 *Frequency-domain responses of the second parametric family with roll-off factor $\alpha = 0.35$*

Lemma 1: The decay rate of the pulse-family in (1) is $1/t^2$ when $\alpha \neq 0$ and $1/|t|$ when $\alpha = 0$.

Proof: In the following, we examine the time-domain properties of acos[acos]. A similar procedure can be applied to all family members under investigation leading to exactly the same conclusion and therefore it is omitted for the sake of brevity. Let us first assume that $\alpha \neq 0$; in this case, it is trivial to show that the derivative of $S_1(f)$ reads (see (6))

For positive frequencies, there are only three transition points that discontinuities may occur, that is $f = B$, $f = B(1-\alpha)$ and $f = B(1+\alpha)$ and therefore it suffices to show that

$$\lim_{f \to B(1+\alpha)^-} S_1'(f) \neq \lim_{f \to B(1+\alpha)^+} S_1'(f) \tag{7}$$

Taking into account that by definition

$$\lim_{f \to B(1+\alpha)^+} S_1'(f) = 0 \tag{8}$$

we can directly focus on the left-hand side term of (7). In other words, let us assume that

$$\lim_{f \to B(1+\alpha)^-} S_1'(f) = T\frac{\gamma_0}{2\alpha B}\left\{\frac{1}{2\gamma}\mathcal{G}'(\gamma_0)\right\} = 0 \tag{9}$$

which leads to $\mathcal{G}'(\gamma_0) = 0$. For the acos[acos] pulse we have

$$\mathcal{G}(f) = \text{acos}(\text{acos}(f)) \tag{10}$$

and thus we can readily obtain

$$\mathcal{G}'(f) = \frac{1}{\sqrt{1-f^2}\sqrt{1-\text{acos}(f)^2}} \tag{11}$$

It can now be observed that

$$\gamma_0 = \mathcal{G}^{-1}(0) = \cos(1) \tag{12}$$

which directly yields $\mathcal{G}'(\gamma_0) \to \infty$. The last equation implies that a discontinuity occurs at

$$f = B(1+\alpha) \tag{13}$$

$$S_1'(f) = \begin{cases} 0, & |f| \leq B(1-\alpha) \\ T\left(\frac{f}{|f|}\right)\left(\frac{\gamma_0}{2\alpha B}\right)\left\{\frac{1}{2\gamma}\mathcal{G}'\left(\frac{\gamma_0}{2\alpha B}(-|f| + B(1+\alpha))\right)\right\}, & B(1-\alpha) < |f| \leq B \\ T\left(\frac{f}{|f|}\right)\left(\frac{\gamma_0}{2\alpha B}\right)\left\{\frac{1}{2\gamma}\mathcal{G}'\left(\frac{\gamma_0}{2\alpha B}(+|f| - B(1-\alpha))\right)\right\}, & B < |f| < B(1+\alpha) \\ 0, & B(1+\alpha) \leq |f| \end{cases} \tag{6}$$

doi: 10.1049/iet-spr.2009.0267

and therefore (7) is satisfied. On the other hand, when $\alpha = 0$ the frequency response degenerates into

$$S_1(f) = \begin{cases} T, & 0 \le |f| \le B \\ 0, & B < |f| \end{cases} \tag{14}$$

which is inherently independent of $\mathcal{G}'(f)$ and its time-domain response becomes

$$s(t) = \mathrm{sinc}(t/T) \tag{15}$$

where $\mathrm{sinc}(x) = \sin x/x$ is the well-known sinc function which decays as $1/|t|$ according to [1, 12]. □

Lemma 2: The members of the pulse family in (5), exhibit exactly the same time-domain characteristics as the pulse family in (1).

Proof: The same procedure can be followed with the only difference lying in the derivative of the frequency response which is now given as (see (16))

In a similar manner, from (8) and (9), it suffices to show that

$$\mathcal{G}'(0) \neq 0 \tag{17}$$

For the acos[exp] we have

$$\mathcal{G}'(f) = -\frac{\exp(f)}{\sqrt{1-\exp(2f)}} \tag{18}$$

while for the asech[exp]

$$\mathcal{G}'(f) = \frac{\tanh(f)}{\sqrt{1-\exp(f)}} \tag{19}$$

In both cases $\mathcal{G}'(0) \to \infty$ which concludes the proof. □

It is worth mentioning that the proposed pulses may decay slower than the RC pulse ($1/t^3$) but this is not essentially a drawback. More specifically, it has been theoretically shown that if the amplitudes of the two largest sidelobes are lower, we can achieve lower BERs for higher values of the excess bandwidth and symbol timing errors [5, 8].

In Figs. 3 and 4, the time-domain responses of both families are, respectively, depicted for a roll-off factor of 0.35. We underline the fact that the pulses defined in the frequency domain in (1) and (5) do not have a closed-form representation in time domain and therefore can be evaluated only numerically.

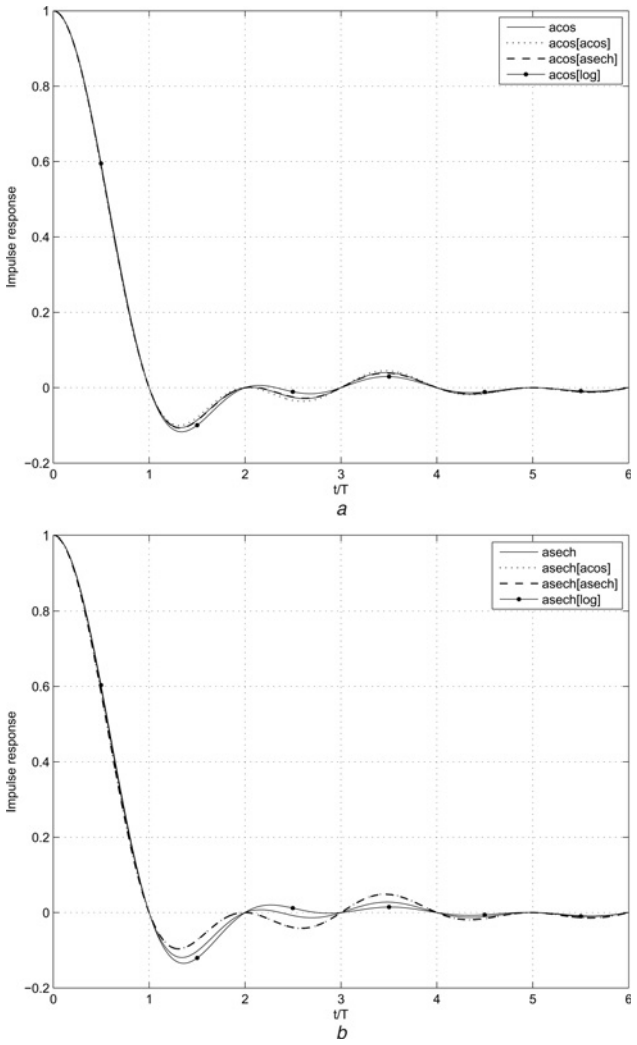

Fig. 3 *Time-domain responses of the first parametric family (acos and asech filters) with roll-off factor $\alpha = 0.35$*

a Acos filters
b Asech filters

4 Performance evaluation

In this section, our main focus is on evaluating the performance of the proposed families using different common figures of merit. We begin with the comparison of the eye diagrams that are a means of visually assessing the vulnerability of transmission systems to the problem of ISI [2]. Owing to space limitations, we consider only the eye diagrams of the first parametric family combined with the acos filters. The corresponding eye patterns, which were generated by superimposing 2^9 distinct binary pulse sequences and observing two consecutive symbol periods, can be seen in Fig. 5; we note that for the sake of clarity, only the inner and outer contour boundaries, corresponding to minimum and maximum distortion have been plotted.

$$S_2'(f) = \begin{cases} 0, & |f| \le B(1-\alpha) \\ T\left(\dfrac{-f}{|f|}\right)\left(\dfrac{1}{2\alpha B}\right)\left\{\dfrac{1}{2\gamma}\mathcal{G}'\left(\dfrac{\gamma_0}{2\alpha B}(+|f| - B(1-\alpha))\right)\right\}, & B(1-\alpha) < |f| \le B \\ T\left(\dfrac{-f}{|f|}\right)\left(\dfrac{1}{2\alpha B}\right)\left\{\dfrac{1}{2\gamma}\mathcal{G}'\left(\dfrac{\gamma_0}{2\alpha B}(-|f| + B(1+\alpha))\right)\right\}, & B < |f| < B(1+\alpha) \\ 0, & B(1+\alpha) \le |f| \end{cases} \tag{16}$$

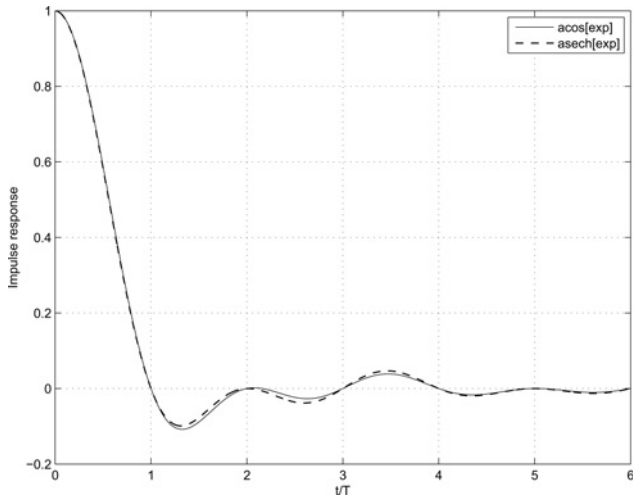

Fig. 4 *Time-domain responses of the second parametric family with roll-off factor $\alpha = 0.35$*

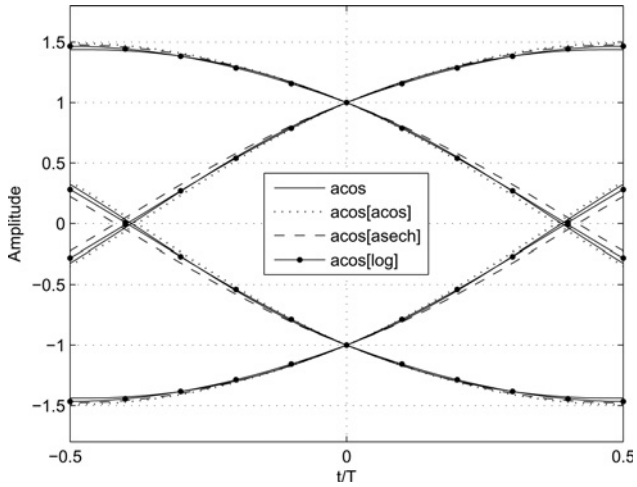

Fig. 5 *Eye diagrams of the first parametric family combined with acos filters for roll-off factor $\alpha = 0.35$*

The largest eye opening is offered by the acos[log], whereas a marginally reduced eye opening is provided by the acos[asech] pulse, which implies a higher level of ISI and, consequently, an increased sensitivity to synchronisation errors [2]. In order to obtain a thorough understanding, the eye width of all the proposed pulses has been estimated at a timing offset of $t/T = 0.5$, as in [12]. The obtained results are depicted in Table 2 (columns 2 and 5). It is interesting to note that, as anticipated, the highest eye opening is offered by the acos[log] pulse followed by the asech[log] pulse. The reference asech pulse may perform better than the majority of the proposed pulses in terms of eye opening but, as it will be shown in the following, it falls short of offering a satisfactorily low BER.

Similar conclusions can be drawn after estimating the maximum distortion experienced by each separate pulse which is, in general, a more quantitative measure of performance (see columns 3 and 6 in Table 2). From a mathematical viewpoint, the maximum distortion is the magnitude of the largest possible ISI sample at any given time instant. In all cases, the point of maximum distortion occurs at $t/T = \pm 0.5$ and the best performance is offered by the acos pulse with the associated value being 1.4387. For the second family, asech[exp] yields a value of 1.5093 and, hence, outperforms acos[exp]. The reference asech pulse yields a maximum distortion of 1.4880, which makes it be outperformed by acos[asech], acos[log] and asech[acos] while the rest pulses yield a relatively higher value of distortion.

The last step of the evaluation process comprises the computation of the average BERs in the presence of time sampling errors. We recall that the BER probability is the ultimate measure of performance that includes the effects of noise, synchronisation and distortion [14]. The error rates have been computed according to [15] for binary antipodal signalling and 2^9 interfering symbols. A system signal-to-noise ratio of 15 dB has been assumed while we have set $M = 45$, $N_1 = -100$, $N_2 = 100$ in [15, equation (41a)] since a further increase in the number of samples does not alter the final results. A theoretical justification for this choice is given in [15]. Note that a similar procedure was also employed in [5–11]. The obtained results are tabulated in Table 3. Generally speaking, timing jitter raises the values of average BER since ISI is a result of the receiver eye being sampled off centre [5]. It can also be easily observed that for the great majority of the values of α and timing jitter, all the proposed pulses yield a smaller BER than asech. This trend is more pronounced for small and moderate values of α and t/T, as commonly encountered in practice.

More importantly, by inspection of Tables 2 and 3, it can be inferred that the best pulse is acos[log] since it yields not only the largest eye opening but also outperforms asech, in terms of average BER, for all the 12 considered cases and maximum distortion. On the other hand, the asech[log] is systematically outperformed by asech and this phenomenon can be attributed to the higher time-domain sidelobes of the former (see Fig. 3*a*) and also to its semi-convex/semi-concave frequency response (see Fig. 1*a*). The rest pulses offer a superior performance for either eleven (acos, acos[acos], acos[asech] and acos[exp]) or ten cases (asech[acos], asech[asech] and asech[exp]), thereby indicating the improved robustness of the proposed families of filters.

Table 2 Eye width and maximum distortion of eye diagrams of all filters

Pulse	Eye width	Max distortion	Pulse	Eye width	Max distortion
acos	0.5365	1.4387	asech	0.5983	1.4880
acos[acos]	0.5211	1.4923	asech[acos]	0.4922	1.4809
acos[asech]	0.5663	1.4770	asech[asech]	0.5113	1.5132
acos[log]	0.6105	1.4663	asech[log]	0.6051	1.5193
acos[exp]	0.4990	1.5256	asech[exp]	0.6030	1.5093

doi: 10.1049/iet-spr.2009.0267

Table 3 Bit error probability of both families of filters for $N = 2^9$ interfering symbols and SNR = 15 dB

α	Pulse	$t/T = \pm 0.05$	$t/T = \pm 0.1$	$t/T = \pm 0.2$	$t/T = \pm 0.3$
0.1	acos	1.1074×10^{-7}	5.4642×10^{-6}	2.0389×10^{-3}	4.5484×10^{-2}
	acos[acos]	1.0917×10^{-7}	5.3024×10^{-6}	1.9764×10^{-3}	4.5015×10^{-2}
	acos[asech]	1.1083×10^{-7}	5.4734×10^{-6}	2.0425×10^{-3}	4.5507×10^{-2}
	acos[log]	1.1407×10^{-7}	5.8218×10^{-6}	2.1749×10^{-3}	4.6428×10^{-2}
	asech	1.1484×10^{-7}	5.9066×10^{-6}	2.2068×10^{-3}	4.6639×10^{-2}
	asech[acos]	1.0802×10^{-7}	5.1873×10^{-6}	1.9316×10^{-3}	4.4662×10^{-2}
	asech[asech]	1.0805×10^{-7}	5.1896×10^{-6}	1.9326×10^{-3}	4.4669×10^{-2}
	asech[log]	1.2292×10^{-7}	6.8472×10^{-6}	2.5495×10^{-3}	4.8699×10^{-2}
	acos[exp]	1.1125×10^{-7}	5.5185×10^{-6}	2.0597×10^{-3}	4.5635×10^{-2}
	asech[exp]	1.0878×10^{-7}	5.2639×10^{-6}	1.9615×10^{-3}	4.4900×10^{-2}
0.35	acos	3.3527×10^{-8}	3.9249×10^{-7}	6.5764×10^{-5}	4.1127×10^{-3}
	acos[acos]	3.2753×10^{-8}	3.7964×10^{-7}	6.4348×10^{-5}	4.0152×10^{-3}
	acos[asech]	3.3558×10^{-8}	3.9255×10^{-7}	6.5582×10^{-5}	4.1067×10^{-3}
	acos[log]	3.5470×10^{-8}	4.3365×10^{-7}	7.3486×10^{-5}	4.5509×10^{-3}
	asech	3.5970×10^{-8}	4.4581×10^{-7}	7.6204×10^{-5}	4.6951×10^{-3}
	asech[acos]	3.2264×10^{-8}	3.7363×10^{-7}	6.4494×10^{-5}	4.0024×10^{-3}
	asech[asech]	3.2255×10^{-8}	3.7275×10^{-7}	6.4110×10^{-5}	3.9850×10^{-3}
	asech[log]	4.2145×10^{-8}	6.2866×10^{-7}	1.2567×10^{-4}	7.0123×10^{-3}
	acos[exp]	3.3806×10^{-8}	3.9786×10^{-7}	6.6617×10^{-5}	4.1638×10^{-3}
	asech[exp]	3.2591×10^{-8}	3.7775×10^{-7}	6.4445×10^{-5}	4.0128×10^{-3}
0.5	acos	2.0431×10^{-8}	1.3300×10^{-7}	1.4717×10^{-5}	1.2578×10^{-3}
	acos[acos]	2.0054×10^{-8}	1.3014×10^{-7}	1.5328×10^{-5}	1.3642×10^{-3}
	acos[asech]	2.0438×10^{-8}	1.3273×10^{-7}	1.4563×10^{-5}	1.2421×10^{-3}
	acos[log]	2.1559×10^{-8}	1.4514×10^{-7}	1.4987×10^{-5}	1.2082×10^{-3}
	asech	2.1875×10^{-8}	1.4917×10^{-7}	1.5345×10^{-5}	1.2253×10^{-3}
	asech[acos]	1.9865×10^{-8}	1.2958×10^{-7}	1.6248×10^{-5}	1.4975×10^{-3}
	asech[asech]	1.9845×10^{-8}	1.2902×10^{-7}	1.6057×10^{-5}	1.4781×10^{-3}
	asech[log]	2.6157×10^{-8}	2.1763×10^{-7}	2.5364×10^{-5}	1.8850×10^{-3}
	acos[exp]	2.0583×10^{-8}	1.3446×10^{-7}	1.4657×10^{-5}	1.2385×10^{-3}
	asech[exp]	1.9992×10^{-8}	1.3005×10^{-7}	1.5658×10^{-5}	1.4094×10^{-3}

5 Conclusion

In this paper, two novel parametric families of ISI-free pulses were proposed that systematically outperform the recently proposed asech pulse. Apart from their improved performance in terms of BER and maximum distortion for the great majority of cases, an important advantage of these families is their high flexibility when it comes down to the construction of a specific pulse shaping filter. Using the acos and asech as the outer functions, it was clearly demonstrated that a plethora of alternatives can be obtained by simply changing the inner functions. All the considered pulses, decay asymptotically as $1/t^2$ unless the roll-off factor is equal to zero when the rate becomes $1/|t|$. While this rate is slower than that of the RC pulse (i.e. $1/t^3$), an improved performance is achieved since the amplitudes of the two higher sidelobes are lower and this results in a smaller BER. We finally highlight that the proposed pulse families require less computational complexity during the design process thanks to the low number of filter parameters.

6 Acknowledgment

Elements of this paper were presented in part at the 2009 International Conference on Communications (ICC), Dresden, Germany, June 2009.

7 References

1 Nyquist, H.: 'Certain topics in telegraph transmission theory', *AIEE Trans.*, 1928, **47**, pp. 617–644

2 Proakis, J.G.: 'Digital communications' (McGraw-Hill, New York, 2000, 4th edn.)

3 Mitola, J.: 'Cognitive radio: an integrated agent architecture for software defined radio'. PhD thesis, Royal Institute of Technology (KTH), Stockholm, Sweden, May 2000

4 Xia, X.: 'A family of pulse-shaping filters with ISI-free matched and unmatched filter properties', *IEEE Trans. Commun.*, 1997, **45**, (10), pp. 1157–1158

5 Beaulieu, N.C., Tan, C.C., Damen, M.O.: 'A "better than" Nyquist pulse', *IEEE Commun. Lett.*, 2001, **5**, (9), pp. 367–368

6 Assalini, A., Tonello, A.M.: 'Improved Nyquist pulses', *IEEE Commun. Lett.*, 2004, **8**, (2), pp. 87–89

7 Chandan, S., Sandeep, P., Chaturvedi, A.K.: 'A family of ISI-free polynomial pulses', *IEEE Commun. Lett.*, 2005, **9**, (6), pp. 496–498

8 Alexandru, N.C.: 'A family of improved Nyquist pulses'. Proc. Int. Symp. on Signals, Circuits and Systems (ISSCS), Romania, July 2007, vol. 2

9 Sandeep, P., Chandan, S., Chaturvedi, A.K.: 'ISI-free pulses with reduced sensitivity to timing errors', *IEEE Commun. Lett.*, 2005, **9**, (4), pp. 292–294

10 Assimonis, S.D., Matthaiou, M., Karagiannidis, G.K.: 'Two-parameter Nyquist pulses with better performance', *IEEE Commun. Lett.*, 2008, **12**, (11), pp. 807–809

11 Assimonis, S.D., Matthaiou, M., Karagiannidis, G.K., Nossek, J.A.: 'Parametric construction of improved Nyquist filters based on inner and outer functions'. Proc. Int. Conf. on Commun., (ICC), Dresden, Germany, June 2009

12 Beaulieu, N.C., Damen, M.O.: 'Parametric construction of Nyquist-I pulses', *IEEE Trans. Commun.*, 2004, **52**, (12), pp. 2134–2142

13 Theodoridis, S., Koutroumbas, K.: 'Pattern recongition' (Acamedic Press, Inc., 2003, 2nd edn.)

14 Tan, C.C., Beaulieu, N.C.: 'Transmission properties of conjugate-root pulses', *IEEE Trans. Commun.*, 2004, **52**, (4), pp. 553–558

15 Beaulieu, N.C.: 'The evaluation of error probabilities for intersymbol and cochannel interference', *IEEE Trans. Commun.*, 1991, **39**, (12), pp. 1740–1749